ingegneria sismica
International Journal of Earthquake Engineering
Anno XLIII - Num. 2 - 2026

Mechanism of the effect of different material combinations on the performance of ice crystals for cold storage

Limin Yuwen[1,*]

[1] State Grid Lang Fang Power Supply Company, Langfang, Hebei, 065099, China

SUMMARY: *Ice crystals for cold storage have extensive applications in modern industry. This paper prepares a novel composite phase-change cold storage material and investigates its optimal mass fraction and performance. Sodium dodecylbenzenesulfonate (SDBS) is used as a dispersant, combined with multilayer graphene, TiO_2/graphene, and TiO_2 particles as thermal conductive additives, incorporated into traditional phase-change cold storage materials. Performance testing through multiple experimental methods revealed that the combination of dispersant and thermal additives did not alter the chemical properties of the cold storage material. The melting and solidification temperatures of the novel composite PFCS material were both 0.88°C. When the material's mass fraction reached 7.5%, its phase change latent heat, phase change temperature, thermal conductivity, cold release efficiency, and transient temperature response rate all demonstrated enhanced effectiveness.*

KEYWORDS: *SDBS; multilayer graphene; TiO_2/graphene; composite phase change thermal storage material; thermal storage ice crystals*

1 Introduction

Human societies have long understood methods for preserving food in low-temperature environments and have also applied low temperatures to other fields such as medicine [1, 2]. Historical records indicate that in the 5th century BC, Hippocrates, the father of Greek medicine, promoted the use of cold therapy for hemostasis. However, the true scientific era of cryopreservation began around the 1950s. In 1949, British biologist Polge serendipitously discovered glycerol's cryoprotective properties for poultry, thereby pioneering the first effective method for preserving living cells and tissues at low temperatures [3, 4]. Since then, cryopreservation technology has been widely adopted across medicine, food storage, biotechnology, and other fields, becoming an indispensable production process in these sectors [5-7].

Cryopreservation technology achieves long-term preservation by artificially creating a low-temperature environment that temporarily slows cellular metabolic rates in viable organisms [8, 9]. As a 21st-century cryopreservation method, cold storage ice crystals have found extensive application in logistics, chilled food preservation, and related fields [10, 11]. However, during the use of cold storage ice crystals, if the quantity is insufficient or the material composition fails to meet standards, the crystals' performance cannot be fully realized, resulting in suboptimal cryopreservation outcomes [12-15]. Conversely, even when material composition requirements are satisfied, excessive use of cold storage ice crystals leading to overperformance can also damage frozen items [16, 17]. Therefore, rationally selecting the material composition

*yuwenlimin@163.com
https://doi.org/10.65102/is2026842
Published: 30 April, 2026

and quantity of phase change materials remains a persistent challenge for researchers and industry professionals [18, 19]. This is primarily because the underlying mechanism of phase change materials is not yet fully understood, making it difficult to develop reasonable and effective formulations and usage methods.

This study prepared novel composite phase change cold storage materials by blending sodium dodecylbenzenesulfonate (SDBS) with multilayer graphene, TiO_2/graphene, and TiO_2 particles, then incorporating them into a binary composite cold storage system (nonanoic acid: decyl alcohol = 70:30). To investigate the material's stability, thermal conductivity, and performance in cold storage and release applications, step cooling tests, differential scanning calorimetry (DSC) experiments, and stability cycling tests were conducted. Through visualization of experimental results and data analysis, the most effective material mass fraction was determined, and the performance changes of the novel composite phase change cold storage material at this mass fraction were studied.

2 Pre-experiment Preparation

2.1 Preparation of Experimental Materials and Sample Preparation

2.1.1 Preparation of Experimental Materials

Multi-layer graphene, Shanghai McLean Biochemical Technology Co., Ltd.; Butyl titanate, TiO_2 particles, Shanghai Jizhi Biochemical Technology Co., Ltd.; Butyl titanate, glacial acetic acid, anhydrous ethanol, dilute HNO_3, nonanoic acid, cetyl alcohol, and sodium dodecylbenzenesulfonate, Nanjing Chemical Reagent Co., Ltd.

2.1.2 Sample Preparation

Preparation of TiO_2/Graphene Composite: Add butyl titanate to a mixture of glacial acetic acid and anhydrous ethanol, stirring thoroughly at room temperature. Mix anhydrous ethanol with deionized water, then adjust the mixture's pH using dilute HNO_3. Ultrasonically disperse graphene into the mixture. Slowly combine the two solutions, stirring for 3 hours at room temperature to obtain a uniform brown sol. Transfer the sol-gel to a hydrothermal reactor and maintain at 220°C for 15 hours. After reaction, allow natural cooling, wash with water until neutral, vacuum filter, and obtain a dry 30% (mass fraction) TiO_2/graphene composite.

This study selected a ratio of m (nonanoic acid): m (myristic alcohol) = 70:30 as the traditional phase change material for thermal storage. Neonic acid and sunflower oil were weighed according to the ratio, with a specific proportion of sodium dodecylbenzenesulfonate (SDBS) dispersant and thermal additives (multi-layer graphene, TiO_2/graphene, and TiO_2 particles) added. The mixture was heated to 60°C in a water bath and stirred for 45 minutes, followed by ultrasonic dispersion for 100 minutes. This process yielded a stable, homogeneous novel composite phase change cold storage material.

2.2 Selection of Experimental Methods

2.2.1 Step-Cooling Test Experiment

Inorganic salts typically exhibit supercooling phenomena, necessitating the measurement of a material's supercooling degree. In step cooling curve experiments, the temperature difference between the inflection point where cooling transitions to heating and the phase transition plateau represents the substance's supercooling degree, while the phase transition plateau

corresponds to the substance's phase transition point. Figure 1 illustrates the step cooling curve process. Key instruments used in the cooling experimental setup for data acquisition include a computer, data acquisition instrument, Type T thermocouple, and cryogenic bath. The Type T thermocouple operates within a common temperature range of -250 to 650°C, characterized by high precision, wide measurement range, and excellent stability. It is employed to monitor temperature changes in thermal storage materials. The data acquisition instrument serves as an automated tool for data collection and conversion. Connected to the thermocouple, it provides real-time, accurate feedback on temperature changes. When linked to a computer, it processes and converts transmitted data for analysis. The cryostat maintains a constant low temperature through circulating water and a temperature control system, providing the necessary cryogenic environment for sample testing.

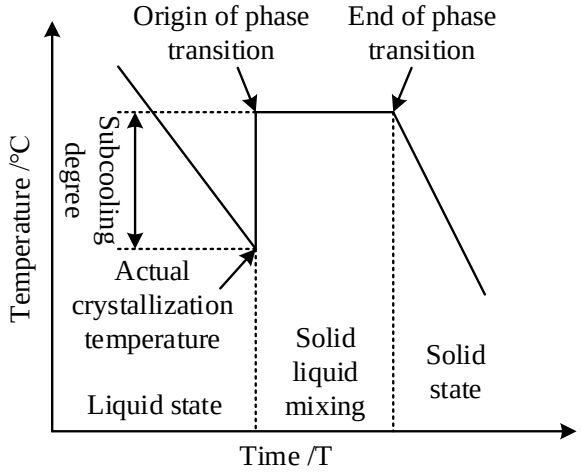

Figure 1: Schematic diagram of the step cold curve

Primary Operating Procedures:

1) Transfer the prepared solution into a 45mL test tube. Seal the tube opening with a silicone stopper to prevent contamination.

2) Position a thermocouple centrally within the test tube to monitor phase change material temperature. Maintain a 1.0-2.0cm distance between the thermocouple and the tube bottom.

3) Activate the cryogenic bath and set its temperature to -25°C.

4) Once the bath stabilizes at -25°C, vertically insert and secure the test tube within the cryostat. Ensure the liquid level of the test material remains below the cryogenic coolant level in the bath.

5) Activate the data acquisition instrument to collect measurements until the sample temperature exhibits a phase transition plateau, indicating the onset of rapid cooling.

6) Halt measurements. Repeat steps 4 and 5 to conduct three replicate experiments.

2.2.2 Differential Scanning Calorimetry

The phase transition characteristic parameters of materials were tested using a differential scanning calorimeter (DSC). These parameters—phase transition temperature, latent heat of phase transition, peak temperature of phase transition, and supercooling—constitute the core aspects of studying phase transition materials. They play a crucial role in understanding the properties of phase transition materials and the phase transition process itself. Measurements were conducted using a Q2000 differential scanning calorimeter (DSC). This instrument employs dynamic zero-balancing theory, with an internal heating mechanism. Both the sample container and the reference object base feature separate supports, each equipped with a platinum

resistance thermometer for heating and a platinum sensor for temperature measurement. During operation, the power of the heating devices for the test sample and reference object is converted under program control. Based on this set value, cooling is applied, and the energy difference of the substance is obtained from its temperature change, forming a DSC curve. This curve reflects the relationship between heat flux and time, enabling analysis of the substance's thermophysical properties.

Primary Operating Steps:

1) In a nitrogen testing environment, set the temperature scan range to -45 to 35°C and program the nitrogen flow rate to 45 mL/min.

2) Eliminate the sample's thermal history through rapid heating and cooling: rapidly decrease from room temperature to -35°C at 25°C/min, hold at -35°C for 2 minutes, then rapidly increase to 25°C at -35°C/min. Repeat this cycle twice before testing the sample.

3) Weigh the sample using an electronic balance to obtain 15–20 mg, accurate to 0.010 mg. Place the sample in a crucible, press it firmly with a presser, and conduct the experiment with the sample placed in the same blank dish.

4) The sample cooling process runs from 25°C to -35°C, and the heating process from -35°C to 25°C. with a heating/cooling rate of 5.0°C/min throughout. Each sample undergoes four tests to obtain freezing and melting curves.

5) Using TA Universal Analysis software, calculate the peak area formed by the curve intersecting the baseline and the maximum slope of the dissolution peak intersecting the baseline. This determines the material's phase transition latent heat and phase transition temperature.

2.2.3 Steady-State Cycling Test

Phase change materials require frequent freezing and thawing during operation. During the low-temperature cold storage phase, the mixed solution cools and crystallizes. Due to differences in solubility, insoluble organic and inorganic substances crystallize at different rates, causing inconsistent precipitation. This leads to phase separation within the same solution. During repeated freeze-thaw cycles, the precipitated substances accumulate progressively, causing increasing density inhomogeneity within the cold storage material. This degradation in properties adversely affects its performance and operational lifespan. The stability of the sample must be determined through low-temperature cycling tests. The primary experimental apparatus includes a computer, data acquisition instrument, T-type thermocouple, and two cryogenic baths.

Main Operational Steps:

1) Transfer the prepared solution into a 45mL test tube. Seal the tube opening with a silicone stopper to prevent contamination.

2) Insert the thermocouple into the center of the test tube to monitor the phase change material's temperature. Maintain a distance of 1.0-2.0cm between the thermocouple and the tube bottom.

3) Activate the first cryostat and set its temperature to -25°C.

4) Once the temperature reaches -25°C and stabilizes, place the test tube vertically into the cryostat and secure it, ensuring the liquid surface of the phase change material remains below the cryostat's cooling fluid level.

5) Activate the data acquisition instrument to collect data until the sample temperature exhibits a phase change plateau, indicating the onset of the rapid cooling phase.

6) Turn on the second cryostat and set its temperature to 25°C.

7) Place the frozen thermal storage material from steps 4 and 5 vertically into the 25°C cryostat.

8) Collect data to obtain the melting curve.

9) Repeat 100 times to complete the stability cycle test.

2.3 Selection of Performance Testing Methods

2.3.1 Thermal Conductivity Testing

Thermal conductivity is a key parameter for evaluating the cold storage rate of phase change materials during use, and it also serves as one basis for assessing the impact of additives on the properties of the original phase change material. Due to the inherent morphological instability of the fabricated composite phase change materials at room temperature, multiple tests are required to objectively evaluate their thermal conductivity. In this study, the DZDR-S thermal conductivity tester was employed to measure the thermal conductivity of the samples.

2.3.2 Cold Storage Performance Testing

The storage and release cooling performance serves as a crucial basis for evaluating phase change thermal storage materials. It not only visually demonstrates differences in thermal conductivity but also reveals their phase transition temperatures. Therefore, this paper considers both thermal conductivity test results and storage/release cooling performance test results as integral components of analyzing the thermal conductivity of phase change thermal storage materials.

Materials were tested using a specially designed storage and release cooling performance platform. Prior to testing, samples were placed inside test tubes. A thermocouple connected to a paperless recorder was positioned at the tube's center, while the container opening was thermally sealed to prevent cold loss. The thermocouple depth within the test tube remained consistent throughout the entire process. The testing procedure is as follows:

1) Preliminary work: Place both test tubes in a freezer to cool and absorb cold energy until their internal temperatures are consistent;

2) Cold release test process: Simultaneously place both test tubes in a hot water bath thermostat pot and record the sample heating rate curve;

3) Cold Storage Test Process: After completing the cooling test, place both test tubes simultaneously in a freezer for cooling. Record the sample cooling rate curve (also known as the step cooling curve).

The experimental procedure involves first heating the material and then cooling it, with temperature curves recorded throughout. To further observe the material's cold storage performance, an additional reheating step was added after the above procedures. This step records the material's temperature changes during the cooling and reheating process.

2.3.3 Transient Temperature Response Test

Transient temperature response is a characterization technique that compares the surface temperature distribution of samples to reflect differences in thermal conductivity. An infrared thermal imager records temperature changes in the sample, primarily analyzing the rate of temperature change through color variations in the surface temperature field and shifts in the central point temperature. Before testing, samples of identical mass (2.0g) are placed into molds of the same diameter (35mm), while two graphene plates are simultaneously heated or cooled to a set temperature. The testing process is as follows:

1) Heating and cooling: The mold containing the composite phase change cooling material was simultaneously placed on the heated graphene plate. The infrared thermal imager recorded the sample status at regular intervals until the center temperatures of both materials reached the graphene plate temperature.

2) Cooling and Cold Storage: Simultaneously place the mold containing the phase change cold storage material on the cooling graphene plate. An infrared thermal imager records the sample status at regular intervals until the center temperatures of both materials cool down to the graphene plate temperature.

Record the transient temperature response behavior of the material during the heating and subsequent cooling process. Perform a cooling followed by heating cycle on the material and record its transient temperature response behavior.

3 Analysis of Experimental Results

3.1 Analysis of Physical Properties of Composite Phase-Change Thermal Storage Materials

3.1.1 Analysis of Switch Reluctance Drive Systems (XRD)

To investigate the cold storage performance of type II composite phase change materials incorporating dispersants and thermal additives, it is first necessary to determine whether they exhibit structural changes at the physical or chemical level, followed by analysis of their cold storage capabilities.

XRD testing was conducted on the composite phase change thermal storage materials. Figure 2 shows the XRD structural spectra of nonanoic acid and heptyl alcohol (N&J), the dispersant (SDBS), the thermal conductive additives (multi-layer graphene, TiO_2/graphene, and TiO_2 particles), and the novel composite phase change thermal storage material. As shown in the figure, the strong peaks corresponding to nonanoic acid and nonyl alcohol, as well as the thermal conductive additives and SDBS, appear at the 2θ positions between 15° and 30° in the new composite PFCEM. No other strong peaks are observed, indicating that adding thermal conductive additives and SDBS to the traditional PFCEM of nonanoic acid and nonyl alcohol does not affect their inherent crystal structures. Therefore, the bonding between nonanoic acid and behenic acid with the thermal conductive additives and SDBS relies primarily on physical interactions rather than chemical reactions forming new substances. This also demonstrates that the novel composite phase change energy storage material prepared via the melt blending method does not alter the inherent properties of nonanoic acid and behenic acid, preserving their excellent phase change energy storage performance and chemical characteristics. Additionally, the weak peak of SDBS indicates its dense structure, enabling it to effectively serve as a supporting material for dispersing and encapsulating the melt. Conversely, the strong peak of the thermal conductive additive suggests that utilizing loose, porous multi-layer graphene, TiO_2/graphene composites, and TiO_2 particles can enhance certain properties of the nonanoic acid and oleic acid materials.

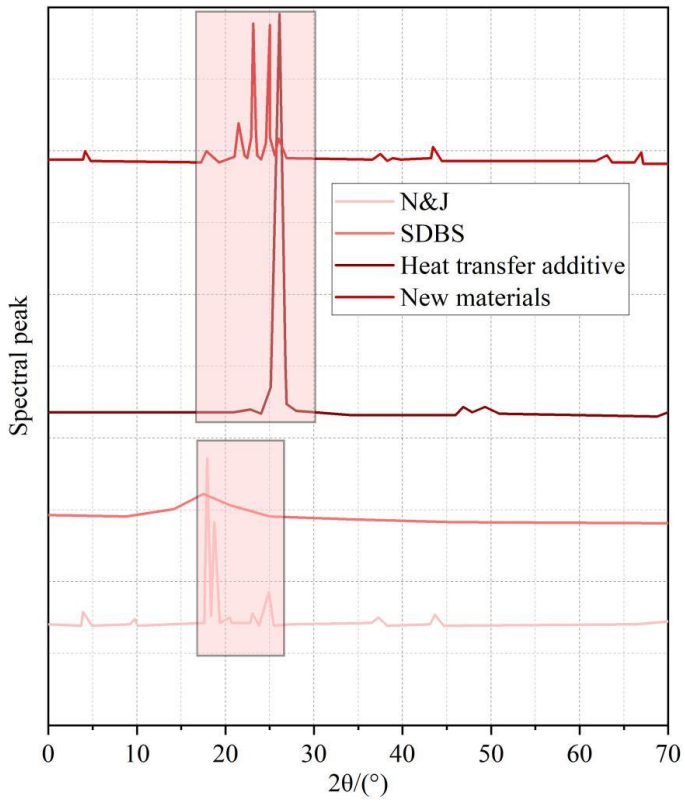

Figure 2: XRD of components of composite phase-change cooling material

3.1.2 Fourier Transform Infrared Spectroscopy (FT-IR) Analysis

Figure 3 shows the Fourier transform infrared spectra of nonanoic acid and heptadecanoic acid (N&J), dispersant (SDBS), thermal conductive additives (multi-layer graphene, TiO_2/graphene, and TiO_2 particles), and the novel composite phase change cold storage material. As shown in the figure, the stretching vibration peaks of methyl and methylene hydrocarbon bonds in nonanoic acid and heptadecanoic acid are located at 3403.28 cm^{-1} and 3324.59 cm^{-1}, respectively. The asymmetric vibrational absorption peak of the methyl group appears at 492.70 cm^{-1}, while the stretching vibration absorption peak of the methyl group is observed at 232.66 cm^{-1}. The infrared absorption curve of the thermal conductive additive is nearly uniform with no absorption peaks. This is because the thermal conductive additive consists of inorganic graphene and its hybrid structural materials, which do not absorb infrared radiation. No additional absorption peaks appeared in the novel composite phase change storage material. The characteristics of both absorption curves were largely similar to those of SDBS with nonanoic acid and oleyl alcohol, indicating no new functional groups formed during composite preparation. The nonanoic acid and oleyl alcohol-thermal conductive additive mixture with SDBS represented a physical blend without chemical reaction. This finding aligns with the XDR results.

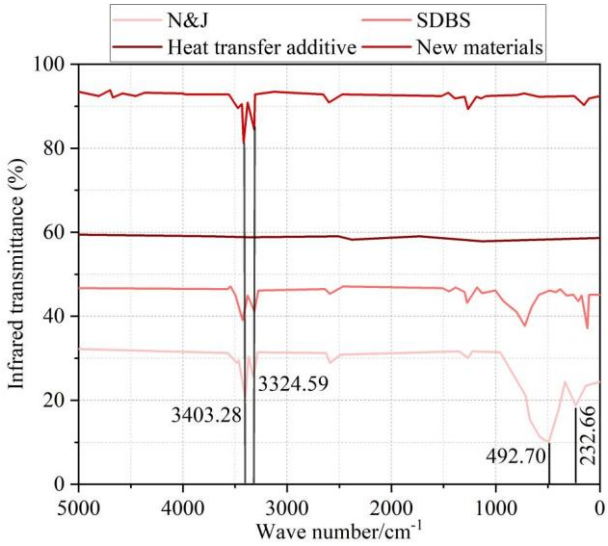

Figure 3: FT-IR of components of composite phase-change cooling material

3.2 Analysis of Experimental Results for Composite Phase-Change Thermal Storage Materials

3.2.1 Differential Scanning Calorimetry Analysis

Differential scanning calorimetry (DSC) analysis was conducted on the novel composite phase change cold storage material. Figure 4 displays the DSC curve of the novel composite phase change cold storage material, encompassing both endothermic (melting) and exothermic (solidification) processes. Both the melting and solidification processes of the novel composite phase change cold storage material exhibit only one distinct peak, attributable to the melting and solidification of the thermal conductive additives within the composite. The melting and solidification temperatures of this novel composite phase change cold storage material are both 0.88°C, with heat flow rates of -26.26 mW and 26.50 mW during melting and solidification, respectively. The prepared novel composite phase change cold storage material demonstrates excellent stability characteristics.

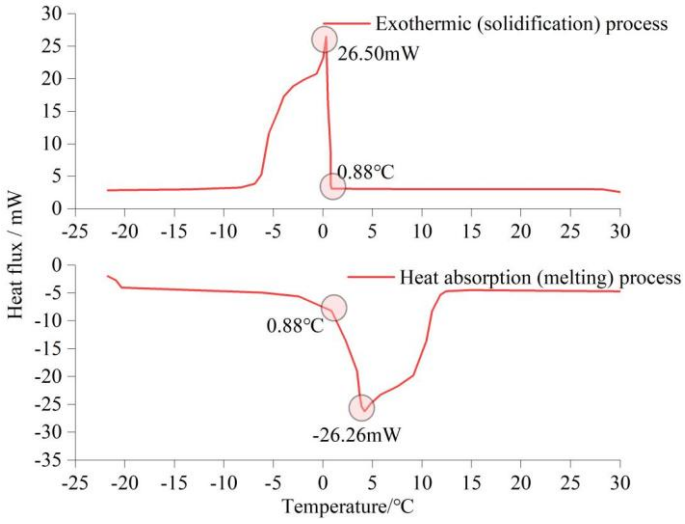

Figure 4: DSC curve of new composite phase-change cooling storage material

3.2.2 Stable Cycle Analysis

In practical applications, phase change materials require frequent freezing and thawing cycles, making stability a critical performance metric. To determine the optimal material mass fraction, this section conducts stability cycling experiments. Figure 5 illustrates the trends of phase change temperature and latent heat as a function of mass fraction for the novel composite phase change storage material. As the mass fraction increases, both latent heat and phase change temperature exhibit a trend of first increasing and then decreasing, with a turning point at 7.5% mass fraction. At a mass fraction of 7.5%, the novel composite phase change cold storage material solution exhibits the maximum latent heat of phase change, reaching 227.545 J/g^{-1}, while the phase change temperature is approximately -3.326°C. Considering the requirements for frequent freezing and thawing cycles, the 7.5% mass fraction solution offers a suitable phase change temperature and substantial latent heat of phase change, thereby enhancing the operational range of cold storage ice crystals.

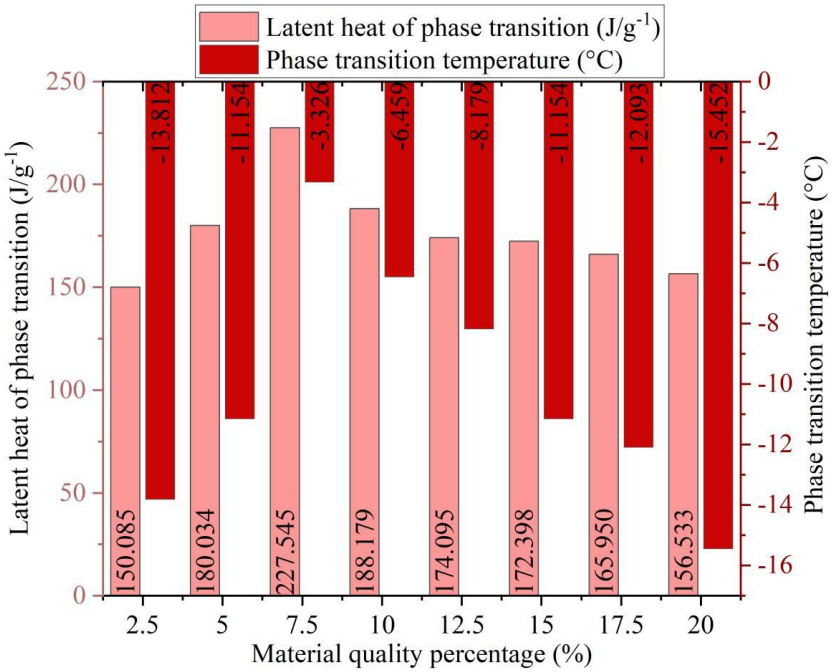

Figure 5: Trend of phase transition temperature and latent heat under different mass

3.2.3 Thermal Conductivity and Cold Storage Performance Analysis

The thermal diffusivity directly influences the heat conduction and cooling release rates of phase change materials during practical applications, serving as a key indicator for evaluating their thermal performance. Thermal diffusivity is affected by thermal conductivity, density, and specific heat capacity. When the thermal diffusivity of a phase change material is low, its temperature transfer occurs slowly, effectively maintaining the material's low-temperature state and reducing heat leakage. Furthermore, during phase transition, the low thermal diffusivity hinders heat transfer from the material to the external environment, significantly reducing heat loss and thereby extending the heat release duration.

Table 1 lists the thermal performance parameters of novel composite phase change cold storage material solutions at different mass fractions. Figure 6 shows the heat release curves of these solutions at varying mass fractions. At a mass fraction of 7.5%, the thermal conductivity λ of the novel composite phase change cold storage material solution is only 0.401 W·m^{-3}·K^{-1}, with a density ρ of just 1.387 g·cm^{-3} and a specific heat capacity c of 2.970 MJ·m^{3}·K^{-1}. The

thermal diffusion coefficient is merely 0.100 $m^{-3}·m^{-1}·K^{-1}$. $(m·K)^{-1}$, with a density ρ of only 1.387 $g·cm^{-3}$, a specific heat capacity c of 2.970 $MJ·(m^3·K)^{-1}$, and a thermal diffusivity coefficient of merely 0.174 $mm^2·s^{-1}$. All four thermal performance parameters reached optimal values. Additionally, the heat release duration for this mass fraction solution reached 100.88 min. The thermal conductivity and heat release performance of the 7.5% mass fraction composite PHSL solution outperform those of other mass fraction solutions.

Table 1: Thermal performance parameters of different mass fraction material

Quality percentage (%)	λ/[W·(m·K)$^{-1}$]	ρ/[g·cm^{-3}]	c/[MJ·(m^3·K)$^{-1}$]	α/[mm^2·s^{-1}]
2.5	0.418	1.413	2.304	0.185
5	0.467	1.465	2.583	0.189
7.5	0.401	1.387	2.970	0.174
10	0.502	1.580	2.641	0.182
12.5	0.493	1.497	2.622	0.176
15	0.461	1.472	2.507	0.168
17.5	0.424	1.463	2.458	0.160
20	0.399	1.401	2.326	0.155

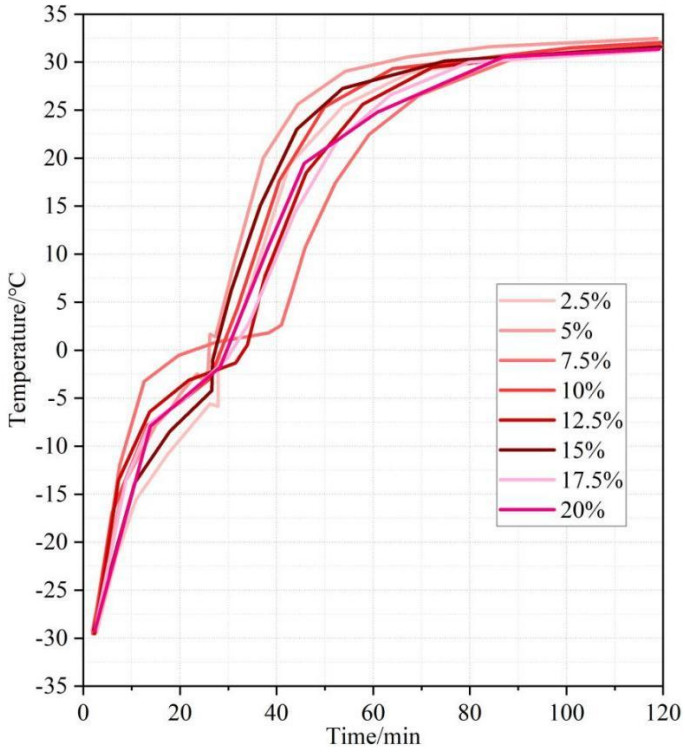

Figure 6: The cooling curves of materials solutions with different mass fractions

3.2.4 Transient Temperature Response Analysis

Transient temperature response tests were conducted on a novel composite phase change cold storage material with a mass fraction of 7.5%. Figure 7 shows the transient temperature response test results for heating release and cooling storage. The response rate for heating and release ranged from 1.032 to 8.541°C/min, while the response rate for cooling and storage ranged from 1.366 to 8.679°C/min. For both heating/release and cooling/storage processes, the new composite phase change thermal storage material exhibited rapid response rates with temperature variations, demonstrating excellent transient temperature response performance.

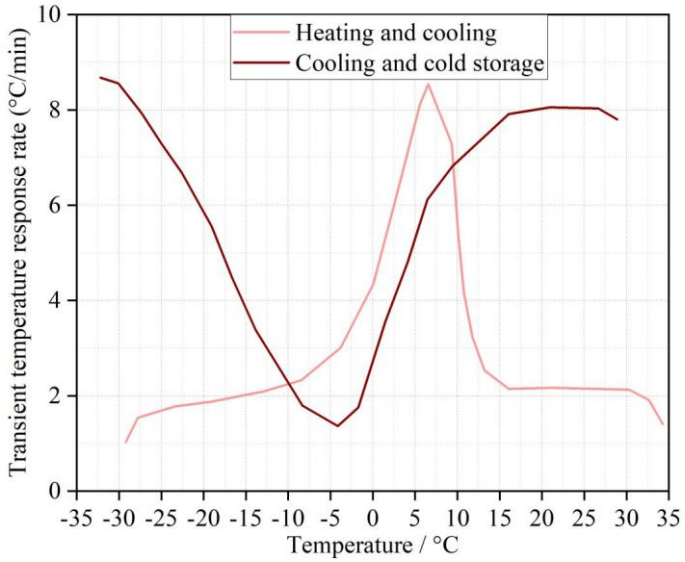

Figure 7: Transient temperature response test results

4 Conclusion

This study investigates the optimal mass fraction and performance variations of a novel composite phase change cold storage material. XRD curves reveal that the strong peaks of the constituent phases appear at 2θ positions between [15,30]°, and combined with FT-IR analysis, it is concluded that this material enhances its properties solely through physical mixing. DSC analysis indicates that both the melting and solidification temperatures of this material are 0.88°C. The novel composite phase change cold storage material with a 7.5% mass fraction exhibits the highest latent heat of phase change (227.545 J/g^{-1}), an optimal phase change temperature (-3.326°C), the lowest thermal diffusivity coefficient (0.174 $mm^2 \cdot s^{-1}$), and the longest heat release duration (100.88 min). This mass fraction of the novel composite phase change cold storage material exhibits rapid transient temperature response rates during both heating/cooling and cooling/storage processes.

References

[1] Owusu-Apenten, R., & Vieira, E. (2022). Low-Temperature Preservation. In Elementary Food Science (pp. 289-316). Cham: Springer International Publishing.

[2] Bai, L., Liu, M., & Sun, Y. (2023). Overview of food preservation and traceability technology in the smart cold chain system. Foods, 12(15), 2881.

[3] Korotkaya, E., KOROTKIY, I., Neverov, E., Sahabutdinova, G., & Monastyrskaya, E. (2022). Biopolymer packaging application for low-temperature food preservation. Periodico tche quimica, 19(41).

[4] Dhanya, R., Panoth, A., & Venkatachalapathy, N. (2024). A comprehensive review on isochoric freezing: a recent technology for preservation of food and non-food items. Sustainable Food Technology, 2(1), 9-18.

[5] Gao, X., Liu, H., Wang, T., Jiang, Z., & Zhu, Y. (2023). Low temperature preservation for

perishable ready to eat foods: Not entirely effective for control of L. monocytogenes. Trends in Food Science & Technology, 142, 104228.

[6] Pan, C., Chen, S., Hao, S., & Yang, X. (2019). Effect of low-temperature preservation on quality changes in Pacific white shrimp, Litopenaeus vannamei: a review. Journal of the Science of Food and Agriculture, 99(14), 6121-6128.

[7] Biglia, A., Comba, L., Fabrizio, E., Gay, P., & Aimonino, D. R. (2016). Case studies in food freezing at very low temperature. Energy Procedia, 101, 305-312.

[8] Joardder, M. U., & Masud, M. H. (2019). Food preservation techniques in developing countries. In Food preservation in developing countries: Challenges and solutions (pp. 67-125). Cham: Springer International Publishing.

[9] Leng, D., Zhang, H., Tian, C., & Xu, H. (2022). Low temperature preservation developed for special foods in East Asia: A review. Journal of Food Processing and Preservation, 46(1), e16176.

[10] Liu, D. K., Xu, C. C., Guo, C. X., & Zhang, X. X. (2020). Sub-zero temperature preservation of fruits and vegetables: A review. Journal of Food Engineering, 275, 109881.

[11] Tolstorebrov, I., Eikevik, T. M., & Bantle, M. (2016). Effect of low and ultra-low temperature applications during freezing and frozen storage on quality parameters for fish. International Journal of Refrigeration, 63, 37-47.

[12] Tan, M., Mei, J., & Xie, J. (2021). The formation and control of ice crystal and its impact on the quality of frozen aquatic products: A review. Crystals, 11(1), 68.

[13] Hunt, C. J. (2019). Technical considerations in the freezing, low-temperature storage and thawing of stem cells for cellular therapies. Transfusion Medicine and Hemotherapy, 46(3), 134-150.

[14] Yu, T., Du, Q., Chen, M., Chen, Y., Song, W., & Feng, Z. (2023). Research progress of mobile cold storage using ice slurry. Energy Storage and Saving, 2(3), 503-512.

[15] Chen, X., Shi, X., Cai, X., Yang, F., Li, L., Wu, J., & Wang, S. (2021). Ice-binding proteins: a remarkable ice crystal regulator for frozen foods. Critical Reviews in Food Science and Nutrition, 61(20), 3436-3449.

[16] Sun, X., Wu, Y., Song, Z., & Chen, X. (2022). A review of natural polysaccharides for food cryoprotection: Ice crystals inhibition and cryo-stabilization. Bioactive Carbohydrates and Dietary Fibre, 27, 100291.

[17] Kang, M., Park, S. Y., Yun, S. M., Chung, H. J., & Chun, H. H. (2024). Effects of sequential combination of cryogenic immersion freezing and ultra-cold frozen storage on the quality of Korean white kimchi. Innovative Food Science & Emerging Technologies, 93, 103642.

[18] Ishevskiy, A. L., & Davydov, I. A. (2017). Freezing as a method of food preservation. Theory and practice of meat processing, 2(2), 43-59

[19] Jia, G., Chen, Y., Sun, A., & Orlien, V. (2022). Control of ice crystal nucleation and growth during the food freezing process. Comprehensive Reviews in Food Science and Food Safety, 21(3), 2433-2454.